

# A line integral-based method to partition climate and catchment effects on runoff

Mingguo Zheng<sup>1, 2\*</sup>

<sup>1</sup>National-Regional Joint Engineering Research Center for Soil Pollution Control and Remediation in South China, Guangdong Key Laboratory of Integrated Agro-environmental Pollution Control and Management, Guangdong Institute of Eco-environmental Science & Technology, Guangdong Academy of Sciences, Guangzhou 510650, China

<sup>2</sup>Guangdong Engineering Center of Non-point Source Pollution Prevention Technology, Guangzhou 510650, China

Correspondence: Mingguo Zheng (mgzheng@soil.gd.cn)

## Abstract

It is a common task to partition the synergistic impacts of drivers in the environmental sciences. However, there is no mathematically precise solution to this partition task. Here I presented a line integral-based method, which addresses the sensitivity to the drivers throughout the drivers' evolutionary paths so as to ensure a precise partition. The method reveals that the partition depends on both the change magnitude and pathway (timing of the change), but not on the magnitude alone unless used for a linear system. To illustrate this method, I applied the Budyko framework to partition the effects of climatic and catchment conditions on the temporal change in the runoff for 19 catchments from Australia and China. The proposed method reduces to the decomposition method when assuming a path in which climate change occurs first, followed by an abrupt change in catchment properties. The proposed method re-defines the widely-used sensitivity at a point as the path-averaged sensitivity. The total differential and the complementary methods simply concern the sensitivity at the initial or/and the terminal state, so they cannot give precise results. Although the path-averaged sensitivities varied greatly among the catchments, they can be readily predicted within the Budyko framework. As a mathematically accurate solution, the proposed method provides a generic tool to conduct quantitative attribution analyses.

**Keywords:** Runoff; Climate change; Human activities; Attribution analysis; Budyko

## 1 Introduction

The impacts of certain drivers on observed changes of interest often require quantification in environmental sciences. In the hydrology community, both climate and human activities have posed global-scale impact on hydrologic cycle and water resources (Barnett *et al.*, 2008; Xu *et al.*, 2014; Wang and Hejazi, 2001). Diagnosing their relative contributions to runoff is of considerable relevance to the researchers and managers. Unfortunately, performing a quantitative attribution analysis of runoff changes remains a challenge (Wang and Hejazi, 2001; Berghuijs and Woods, 2016; Zhang *et al.*, 2016);

40 this is to a considerable degree due to a lack of a mathematically precise method to decouple synergistic  
41 and often confounding impacts of climate change and human activities.

42 Numerous studies have detected the long-term variability in runoff and attempted to partition the  
43 effects of climate change and human activities through various methods (Dey and Mishra, 2017); these  
44 include the paired-catchments method and the hydrological modeling method. The paired-catchment  
45 method can filter the effect of climatic variability and thus isolate the runoff change induced by  
46 vegetation changes (Brown *et al.*, 2005). However, this method is capital intensive; moreover, it  
47 generally involves small catchments and experiences difficulties when extrapolating to large catchments  
48 (Zhang *et al.*, 2011). The physical-based hydrological models often have limitations such as a high data  
49 requirement, labor-intensive calibration and validation processes, and inherent uncertainty and  
50 interdependence in parameter estimations (Binley *et al.*, 1991; Wang *et al.*, 2013; Liang *et al.*, 2015).  
51 Conceptual models such as Budyko-type equations (see Section 2.1) have consequently gained interest  
52 in recent years.

53 Within the Budyko framework, studies (Roderick and Farquhar, 2011; Zhang *et al.*, 2016) have  
54 used the total differential of runoff as a proxy for the runoff change and the partial derivatives as the  
55 sensitivities (hereafter called the total differential method). The total differential, however, is simply a  
56 first-order approximation of the observed change (Fig. 1(a)). This approximation has caused an error in  
57 the calculation of climate impact on runoff, with the deviation ranging from 0 to 20  $10^{-3}$ m (or -118 to  
58 174%) in China (Yang *et al.*, 2014). The elasticity method proposed by Schaake (1990) is also based on  
59 the total differential expression (Sankarasubramanian *et al.*, 2001; Zheng *et al.*, 2009). The method uses  
60 the “elasticity” concept to assess the climate sensitivity of runoff. The elasticity coefficients, however,  
61 have been estimated in an empirical way and are not physically sound (Roderick and Farquhar, 2011;  
62 Liang *et al.*, 2015).

63 The so-called decomposition method developed by Wang and Hejazi (2011) has also been  
64 widely used. The method assumes that climate changes cause a shift along a Budyko curve and then  
65 human interferences cause a vertical shift from one Budyko curve to another (Fig. 2). Under this  
66 assumption, the method extrapolates the Budyko models that are calibrated using observations of the  
67 reference period, in which human impacts remain minimal, to determine the human-induced runoff  
68 changes that occur during the evaluation period.

69 Recently, Zhou *et al.* (2016) established a Budyko complementary relationship for runoff and  
70 further applied it to partitioning the climate and catchment effects. Superior to the total differential  
71 method, the complementary method culminates by yielding a no-residual partition. Nevertheless, this  
72 method depends on a given weighted factor that is determined in an empirical but not a precise way.  
73 Furthermore, Zhou *et al.* (2016) argued that the partition is not unique in the Budyko framework  
74 because the path of the climate and catchment changes cannot be uniquely identified.

75 Obtaining a precise partition remains difficult, even when giving a precise mathematical model.  
76 This difficulty can be illustrated by using a precise hydrology model  $R = f(x, y)$ , where  $R$  represents  
77 runoff, and  $x$  and  $y$  represent the climate factors and catchment characteristics, respectively. We  
78 assumed that  $R$  changes by  $\Delta R$  when  $x$  changed by  $\Delta x$  and  $y$  changes by  $\Delta y$ , *i.e.*,  
79  $\Delta R = f(x + \Delta x, y + \Delta y) - f(x, y)$ . To determine the effect of  $x$  on  $\Delta R$ , *i.e.*  $\Delta R_x$ , a common practice is to  
80 assume that  $y$  remains constant when  $x$  changes by  $\Delta x$ . We thus obtain:  $\Delta R_x = f(x + \Delta x, y) - f(x, y)$ .

81 Similarly, we can obtain:  $\Delta R_y = f(x, y + \Delta y) - f(x, y)$ . Although this derivation seems quite reasonable, it  
 82 is problematic as  $\Delta R_x + \Delta R_y \neq \Delta R$ . A further examination shows that a variable's effect on  $R$  seems to  
 83 differ depending on the changing path (timing of the change). For example,  $\Delta R_x = f(x + \Delta x, y) - f(x, y)$   
 84 and  $\Delta R_y = f(x + \Delta x, y + \Delta y) - f(x + \Delta x, y)$  if  $x$  changes first and  $y$  subsequently changes (Note that the  
 85 partition is precise with  $\Delta R_x + \Delta R_y = \Delta R$  at this moment). If  $y$  changes first and  $x$  subsequently changes,  
 86 the partition then becomes:  $\Delta R_x = f(x + \Delta x, y + \Delta y) - f(x, y + \Delta y)$  and  $\Delta R_y = f(x, y + \Delta y) - f(x, y)$ . In the  
 87 case of  $x$  and  $y$  changing simultaneously, unfortunately, current literature seems not to provide a  
 88 mathematically precise solution.

89 The aim of this study is to propose a mathematically precise method to conduct a quantitative  
 90 attribution to drivers. The method is based on the line integer (called the LI method hereafter) and takes  
 91 account of the sensitivity throughout the evolutionary path of the drivers rather than at a point as the  
 92 total differential method does. To present and evaluate the proposed method, I decomposed the relative  
 93 influences of climate and catchment conditions on runoff within the Budyko framework using data from  
 94 19 catchments from Australia and China.

95

## 96 2 Methodology

### 97 2.1 Budyko Framework and the MCY equation

98 Budyko (1974) argued that the mean annual evapotranspiration ( $E$ ) is largely determined by the  
 99 water and energy balance of a catchment. Using precipitation ( $P$ ) and potential evapotranspiration ( $E_0$ )  
 100 as proxies for water and energy availabilities respectively, the Budyko framework  
 101 relates evapotranspiration losses to the aridity index defined as the ratio of  $E_0$  over  $P$ . The Budyko  
 102 framework has gained wide acceptance in the hydrology community (Berghuijs and Woods, 2016;  
 103 Sposito, 2017). In recent decades, several equations have been developed to describe the Budyko  
 104 framework. Among them, the Mezentsev-Choudhury-Yang's equation (Mezentsev, 1955; Choudhury,  
 105 1999; Yang *et al.*, 2008) (Called the MCY equation hereafter) has been widely accepted and was used  
 106 in this study:

$$107 \quad \frac{E}{P} = \frac{E_0/P}{(1 + (E_0/P)^n)^{1/n}} \quad (1)$$

108 where  $n \in (0, \infty)$  is an integration constant that is dimensionless, and represents catchment properties. Eq.  
 109 (3) requires a relatively long time scale whereby the water storage of a catchment is negligible and the  
 110 water balance equation reduces to be  $R = P - E$ . Here I adopted a "tuned"  $n$  value that can obtain an  
 111 exact accordance between the calculated  $E$  by Eq. (1) and that actually encountered ( $= P - R$ ).

112 The partial differentials of  $R$  with respect to  $P$ ,  $E_0$ , and  $n$  are given as:

$$113 \quad \frac{\partial R}{\partial P} = R_P(P, E_0, n) = 1 - \frac{E_0^{n+1}}{(P^n + E_0^n)^{1/n}} \quad (2a)$$

$$114 \quad \frac{\partial R}{\partial E_0} = R_{E_0}(P, E_0, n) = -\frac{P^{n+1}}{(P^n + E_0^n)^{1/n}} \quad (2b)$$

$$\frac{\partial R}{\partial n} = R_n(P, E_0, n) = \frac{-E_0 P n^{-1}}{(P^n + E_0^n)^{1/n}} \left[ \frac{\ln(P^n + E_0^n)}{n} - \frac{P^n \ln P + E_0^n \ln E_0}{P^n + E_0^n} \right] \quad (2c)$$

## 116 2.2 Theory of the line integral-based method

117 We start by considering an example of a two-variable function  $z = f(x, y)$  and assumed that  $x$  and  
 118  $y$  are independent. The function has continuous partial derivatives  $\partial z / \partial x = f_x(x, y)$  and  $\partial z / \partial y = f_y(x, y)$ .  
 119 Suppose that  $x$  and  $y$  vary along a smooth curve  $L$  (e.g.  $AC$  in Fig. 3) from the initial state  $(x_0, y_0)$  to the  
 120 terminal state  $(x_N, y_N)$ , and  $z$  co-varies from  $z_0$  to  $z_N$ . Let  $\Delta z = z_N - z_0$ ,  $\Delta x = x_N - x_0$ , and  $\Delta y = y_N - y_0$ .  
 121 Our goal is to determine a mathematical solution that quantifies the effects of  $\Delta x$  and  $\Delta y$  on  $\Delta z$ , *i.e.*  
 122  $\Delta z_x$  and  $\Delta z_y$ .  $\Delta z_x$  and  $\Delta z_y$  should be subject to the constraint  $\Delta z_x + \Delta z_y = \Delta z$ .

123 As shown in Fig. 3, points  $M_1(x_1, y_1), \dots, M_{N-1}(x_{N-1}, y_{N-1})$  partition  $L$  into  $N$  distinct segments. Let  
 124  $\Delta x_i = x_{i+1} - x_i$ ,  $\Delta y_i = y_{i+1} - y_i$ , and  $\Delta z_i = z_{i+1} - z_i$ . For each segment,  $\Delta z_i$  can be approximated as  $dz_i$ :  
 125  $\Delta z_i \approx dz_i = f_x(x_i, y_i)\Delta x_i + f_y(x_i, y_i)\Delta y_i$ . We then have:  $\Delta z = \sum_{i=1}^N \Delta z_i \approx \sum_{i=1}^N f_x(x_i, y_i)\Delta x_i + \sum_{i=1}^N f_y(x_i, y_i)\Delta y_i$ . We  
 126 thus obtain the following respective approximation of  $\Delta z_x$  and  $\Delta z_y$ :  $\Delta z_x \approx \sum_{i=1}^N f_x(x_i, y_i)\Delta x_i$  and

127  $\Delta z_y \approx \sum_{i=1}^N f_y(x_i, y_i)\Delta y_i$ . Next, define  $\tau$  as the maximum length of the  $N$  segments. The smaller the value of

128  $\tau$ , the closer to  $\Delta z_i$  the value of  $dz_i$ , and then the more accurate the approximations are. The  
 129 approximations become exact in the limit  $\tau \rightarrow 0$ . Taking the limit  $\tau \rightarrow 0$  then converts the sum into  
 130 integrals and gives a precise expression (this is an informal derivation and please see Appendix A for a

131 formal one):  $\Delta z = \lim_{\tau \rightarrow 0} \sum_{i=1}^N f_x(x_i, y_i)\Delta x_i + \lim_{\tau \rightarrow 0} \sum_{i=1}^N f_y(x_i, y_i)\Delta y_i = \int_L f_x(x, y)dx + \int_L f_y(x, y)dy$ , where

132  $\int_L f_x(x, y)dx = \lim_{\tau \rightarrow 0} \sum_{i=1}^N f_x(x_i, y_i)\Delta x_i$  and  $\int_L f_y(x, y)dy = \lim_{\tau \rightarrow 0} \sum_{i=1}^N f_y(x_i, y_i)\Delta y_i$  denote the line integral of  $f_x$  and  $f_y$

133 along  $L$  (termed integral path) with respect to  $x$  and  $y$ , respectively.  $\int_L f_x(x, y)dx$  and  $\int_L f_y(x, y)dy$  exist  
 134 provided that  $f_x$  and  $f_y$  are continuous along  $L$ . We thus obtain a precise evaluation of  $\Delta z_x$  and  $\Delta z_y$ :

$$135 \Delta z_x = \int_L f_x(x, y)dx \quad (3a)$$

$$136 \Delta z_y = \int_L f_y(x, y)dy. \quad (3b)$$

137 Unlike the total differential method, the sum of  $\Delta z_x$  and  $\Delta z_y$  persistently equals  $\Delta z$  (Appendix B).  
 138 If  $f(x, y)$  is linear, then  $f_x$  and  $f_y$  are constant. Defining  $f_x(x, y)$  and  $f_y(x, y)$  remain constant at  $C_x$  and  $C_y$   
 139 respectively, then  $\Delta z_x = C_x \Delta x$  and  $\Delta z_y = C_y \Delta y$ .  $\Delta z_x$  and  $\Delta z_y$  are thus independent of  $L$ . If  $f(x, y)$  is non-linear,  
 140 however, both  $\Delta z_x$  and  $\Delta z_y$  vary with  $L$ , as is exemplified in Appendix C. Hence, the initial and the  
 141 terminal states, together with the path connecting them, determine the resultant partition unless  $f(x, y)$  is  
 142 linear.

143 The mathematical derivation above applies to a three-variable function as well. By doing the line  
 144 integrals for the MCY equation, we obtain the desired results:

$$145 \quad \Delta R_P = \int_L \frac{\partial R}{\partial P} dP \quad (4a)$$

$$146 \quad \Delta R_{E_0} = \int_L \frac{\partial R}{\partial E_0} dE_0 \quad (4b)$$

$$147 \quad \Delta R_n = \int_L \frac{\partial R}{\partial n} dn \quad (4c)$$

148 where  $\Delta R_P$ ,  $\Delta R_{E_0}$ , and  $\Delta R_n$  denote the effects on runoff change of  $P$ ,  $E_0$ , and  $n$ , respectively. The sum of  
 149  $\Delta R_P$  and  $\Delta R_{E_0}$  represents the effect of climate change, and  $\Delta R_n$  is often related to human activities  
 150 although it probably includes the effects of other factors, such as climate seasonality (Roderick and  
 151 Farquhar, 2011; Berghuijs and Woods, 2016).  $L$  denotes a three-dimensional curve along which climate  
 152 and catchment changes have occurred. I approximated  $L$  by a series of line segments.  $\Delta R_P$ ,  $\Delta R_{E_0}$ , and  $\Delta R_n$   
 153 were finally determined by summing up the integrals along each of the line segments (see Section 2.3).

### 154 2.3 Using the LI method to determine $\Delta R_P$ , $\Delta R_{E_0}$ , and $\Delta R_n$ within the Budyko Framework

#### 155 1) Determining $\Delta R_P$ , $\Delta R_{E_0}$ , and $\Delta R_n$ assuming a linear integral path

156 A curve can always be approximated as a series of line segments. Hence, we can first handle  
 157 the case of a linear integral path. Given two consecutive periods and assuming that the catchment state  
 158 has evolved from  $(P_1, E_{01}, n_1)$  to  $(P_2, E_{02}, n_2)$  along a straight line  $L$ , let  $\Delta P = P_2 - P_1$ ,  $\Delta E_0 = E_{02} - E_{01}$ ,  
 159 and  $\Delta n = n_2 - n_1$ ; then the line  $L$  is given by parametric equations:  $P = \Delta Pt + P_1$ ,  $E_0 = \Delta E_0 t + E_{01}$ ,  
 160  $n = \Delta n t + n_1$ ,  $t \in [0, 1]$ . Given these equations, Eq. (2) becomes a univariate function of  $t$ , *i.e.*,  
 161  $\partial R / \partial P = R_P(t)$ ,  $\partial R / \partial E_0 = R_{E_0}(t)$ , and  $\partial R / \partial n = R_n(t)$ . Then,  $\Delta R_P$ ,  $\Delta R_{E_0}$ , and  $\Delta R_n$  can be evaluated as:

$$162 \quad \Delta R_P = \int_L \frac{\partial R}{\partial P} dP = \int_0^1 R_P(t) d(\Delta Pt + P_1) = \Delta P \int_0^1 R_P(t) dt \quad (5a)$$

$$163 \quad \Delta R_{E_0} = \int_L \frac{\partial R}{\partial E_0} dE_0 = \int_0^1 R_{E_0}(t) d(\Delta E_0 t + E_{01}) = \Delta E_0 \int_0^1 R_{E_0}(t) dt \quad (5b)$$

$$164 \quad \Delta R_n = \int_L \frac{\partial R}{\partial n} dn = \int_0^1 R_n(t) d(\Delta n t + n_1) = \Delta n \int_0^1 R_n(t) dt \quad (5c)$$

165 Unfortunately, I could not determine the antiderivatives of  $R_P(t)dt$ ,  $R_{E_0}(t)dt$  and  $R_n(t)dt$  and had  
 166 to make approximate calculations. As the discrete equivalent of integration is a summation, we can  
 167 approximate the integration as a summation. I divided the  $t \in [0, 1]$  interval into 1000 subintervals of the  
 168 same width, *i.e.*, setting  $dt$  identically equal to 0.001, and then calculated  $R_P(t)dt$ ,  $R_{E_0}(t)dt$  and  $R_n(t)dt$  for  
 169 each subinterval. Let  $t_i = 0.001i$ ,  $i \in [0, 999]$  and is integer-valued.  $\Delta R_P$ ,  $\Delta R_{E_0}$ , and  $\Delta R_n$  are approximated as:

$$170 \quad \Delta R_P \approx 0.001 \Delta P \sum_{i=0}^{999} R_P(t_i) \quad (6a)$$

$$171 \quad \Delta R_{E_0} \approx 0.001 \Delta E_0 \sum_{i=0}^{999} R_{E_0}(t_i) \quad (6b)$$

$$\Delta R_n \approx 0.001 \Delta n \sum_{i=0}^{999} R_n(t_i) \quad (6c)$$

## 2) Dividing the evaluation period into a number of subperiods

I first determined a change point and divided the whole observation period into the reference and evaluation periods. To determine the integral path, the evaluation period was further divided into a number of subperiods. The Budyko framework assumes a steady state condition of a catchment and therefore requires no change in soil water storage. Over a time period of 5-10 years, it is reasonable to assume that changes in soil water storage will be sufficiently small (Zhang *et al.*, 2001). Here, I divided the evaluation period into a number of 7-year subperiods with the exception for the final subperiod, which varied from 7 to 13 years in length depending on the length of the evaluation period.

## 3) Determining $\Delta R_p$ , $\Delta R_{E_0}$ , and $\Delta R_n$ by approximating the integral path as a series of line segments

For a short period, the integral path  $L$  can be considered as linear, which implies a temporally invariant change rate. For a long period in which the change rate varies over time,  $L$  can be fitted using a number of line segments. Given a reference period and an evaluation period comprising  $N$  subperiods, the catchment state was assumed to evolve from  $(P_0, E_{00}, n_0)$ , ...,  $(P_i, E_{0i}, n_i)$ , ..., to  $(P_N, E_{0N}, n_N)$ , where the subscript "0" denotes the reference period, and "i" and "N" denote the  $i$ th and the final subperiods of the evaluation period, respectively. I used a series of line segments  $L_1, L_2, \dots, L_N$  to approximate the integral path  $L$ , where  $L_i$  connects points  $(P_{i-1}, E_{0,i-1}, n_{i-1})$  with  $(P_i, E_{0i}, n_i)$ . Then  $\Delta R_p$ ,  $\Delta R_{E_0}$ , and  $\Delta R_n$  were evaluated as the sum of the integrals along each of the line segments, which were calculated using Eq. (6).

## 2.4 Total-differential, decomposition and complementary methods

To evaluate the LI method, I compared it with the existing methods, including the decomposition method, the total differential method, and the complementary method. The total differential method approximated  $\Delta R$  as  $dR$ :

$$\Delta R \approx dR = \frac{\partial R}{\partial P} \Delta P + \frac{\partial R}{\partial E_0} \Delta E_0 + \frac{\partial R}{\partial n} \Delta n = \lambda_P \Delta P + \lambda_{E_0} \Delta E_0 + \lambda_n \Delta n \quad (7)$$

where  $\lambda_P = \partial R / \partial P$ ,  $\lambda_{E_0} = \partial R / \partial E_0$ , and  $\lambda_n = \partial R / \partial n$ , representing the sensitivity coefficient of  $R$  with respect to  $P$ ,  $E_0$ , and  $n$ , respectively. Within the total differential method,  $\Delta R_p = \lambda_P \Delta P$ ,  $\Delta R_{E_0} = \lambda_{E_0} \Delta E_0$ , and  $\Delta R_n = \lambda_n \Delta n$ . I used the forward approximation, *i.e.*, substituting the observed mean annual values of the reference period into Eq. (2), to estimate  $\lambda_P$ ,  $\lambda_{E_0}$ , and  $\lambda_n$ , as is standard in most studies (Roderick and Farquhar, 2011; Yang and Yang, 2011; Sun *et al.*, 2014).

The decomposition method (Wang and Hejazi, 2011) calculated  $\Delta R_n$  as follows:

$$\Delta R_n = R_2 - R_2' = (P_2 - E_2) - (P_2 - E_2') = E_2' - E_2 \quad (8)$$

where  $R_2$ ,  $P_2$ , and  $E_2$  represents the mean annual runoff, precipitation and evapotranspiration of the evaluation period, respectively;  $R_2'$  and  $E_2'$  represent the mean annual runoff and evapotranspiration, respectively, given the climate conditions of the evaluation period and the catchment conditions of the reference period (Fig. 2). Both  $E_2$  and  $E_2'$  were calculated by Eq. (1), but using  $n$  values of the evaluation period and the reference period respectively.

208 The complementary method (Zhou *et al.*, 2016) uses a linear combination of the complementary  
 209 relationship for runoff to determine  $\Delta R_p$ ,  $\Delta R_{E_0}$ , and  $\Delta R_n$  :

$$210 \quad \Delta R = a \left[ \left( \frac{\partial R}{\partial P} \right)_1 \Delta P + \left( \frac{\partial R}{\partial E_0} \right)_1 \Delta E_0 + P_2 \Delta \left( \frac{\partial R}{\partial P} \right) + E_{0,2} \Delta \left( \frac{\partial R}{\partial E_0} \right) \right] \quad (9)$$

$$+ (1-a) \left[ \left( \frac{\partial R}{\partial P} \right)_2 \Delta P + \left( \frac{\partial R}{\partial E_0} \right)_2 \Delta E_0 + P_1 \Delta \left( \frac{\partial R}{\partial P} \right) + E_{0,1} \Delta \left( \frac{\partial R}{\partial E_0} \right) \right]$$

211 where the subscript 1 and 2 denotes the reference and the evaluation periods, respectively.  $a$  is a  
 212 weighting factor and varies from 0 to 1. As suggested by Zhou *et al.* (2016), I set  $a = 0.5$ . Equation (9)  
 213 thus gave an estimation of  $\Delta R_p$ ,  $\Delta R_{E_0}$ , and  $\Delta R_n$  as follows:

$$214 \quad \Delta R_p = 0.5 \Delta P \left[ \left( \frac{\partial R}{\partial P} \right)_1 + \left( \frac{\partial R}{\partial P} \right)_2 \right] \quad (10a)$$

$$215 \quad \Delta R_{E_0} = 0.5 \Delta E_0 \left[ \left( \frac{\partial R}{\partial E_0} \right)_1 + \left( \frac{\partial R}{\partial E_0} \right)_2 \right] \quad (10b)$$

$$216 \quad \Delta R_n = 0.5 \Delta \left( \frac{\partial R}{\partial P} \right) (P_1 + P_2) + 0.5 \Delta \left( \frac{\partial R}{\partial E_0} \right) (E_{0,1} + E_{0,2}) \quad (10c)$$

## 217 2.5 Data

218 I collected runoff and climate data from 19 selected catchments evaluated in previous studies  
 219 (Table 1). The change-point years given in these studies were directly used to determine the reference  
 220 and evaluation periods for the LI method. As mentioned above, the LI method further divides the  
 221 evaluation period into a number of subperiods. For the sake of comparison, the final subperiod of the  
 222 evaluation period was used as the evaluation period for the decomposition, the total differential and the  
 223 complementary methods (It can be equally considered that all of the four methods used the final  
 224 subperiod as the evaluation period, but the LI method cares about the intermediate period between the  
 225 reference and the evaluation periods and the other methods do not). Eight of the 19 catchments had a  
 226 reference period comprising only one subperiod (Table 1), and the others had two to seven subperiods.

227 The 19 selected catchments have diverse climates and landscapes with 12 from Australia and  
 228 seven from China (Table 1). The catchments span from tropical to subtropical and temperate areas and  
 229 from humid to semi-humid and semiarid regions, with the mean annual rainfall varying from 506 to  
 230 1014  $10^{-3}$ m and potential evaporation from 768 to 1169  $10^{-3}$ m. The dryness index ranges between 0.86  
 231 and 1.91. The catchment areas vary by five orders of magnitude from 1.95 to 121,972 with a median  
 232 606  $10^6$ m<sup>2</sup>. The key data includes annual runoff, precipitation, and potential evaporation. The record  
 233 length varied between 19 and 76 with a median of 39 years. All the catchments experienced changes in  
 234 climate and catchment properties over the observation periods. The precipitation changes from the  
 235 reference to the evaluation period ranged between -153 and 79  $10^{-3}$ m yr<sup>-1</sup>, and between -35 and 41  $10^{-3}$   
 236 m yr<sup>-1</sup> for potential evaporation (Table 2). The coeval change in the parameter  $n$  of the MCY equation  
 237 ranged between -0.2 to 1.4. The mean annual streamflow reduced for all catchments, ranging from 0.4  
 238 to 169 with a median 38  $10^{-3}$ m yr<sup>-1</sup>. The change in catchment properties mainly refer to the vegetation  
 239 cover or land use change. More details of data and the catchments can be found in Zhang *et al.* (2011),  
 240 Sun *et al.* (2014), Zhang *et al.* (2010), Zheng *et al.* (2009), Jiang *et al.* (2015), and Gao *et al.* (2016).

### 242 3 Results

243 Table 3 lists the resultant values of  $\Delta R_p$ ,  $\Delta R_{E_0}$ , and  $\Delta R_n$  from the LI method and the three other  
 244 methods. Please see the supplemental information section for detailed calculation steps.

245 Fig. 4(a) compares the resultant  $\Delta R_n$  of the LI method and the decomposition method. Although  
 246 they are quite similar, the discrepancies can be up to  $>20 \cdot 10^{-3} \text{m yr}^{-1}$ . The decomposition method  
 247 assumes that climate change occurs first and then human interferences cause a sudden change in  
 248 catchment properties (Fig. 2). Such a fictitious path is identical to the path ABC in Fig. 3, provided that  
 249  $x$  represents climate factors and  $y$  catchment properties. When adopting ABC as the integral path, the LI  
 250 method yielded the same results as the decomposition method did (Fig. 4(b)). Hence, the decomposition  
 251 method can be considered as a case of the LI method that uses a special integral path.

252 The total differentiae method is predicated on an approximate equation, *i.e.* Eq. (7). The LI  
 253 method reveals that the precise form of the equation is  $\Delta R = \overline{\lambda_P} \Delta P + \overline{\lambda_{E_0}} \Delta E_0 + \overline{\lambda_n} \Delta n$  (Appendix D), where  
 254  $\overline{\lambda_P}$ ,  $\overline{\lambda_{E_0}}$  and  $\overline{\lambda_n}$  denote the path-averaged sensitivity of  $R$  to  $P$ ,  $E_0$ , and  $n$ , respectively. All points along  
 255 the path have the same weight in determining  $\overline{\lambda_P}$ ,  $\overline{\lambda_{E_0}}$  and  $\overline{\lambda_n}$ . To determine them, the total differential and  
 256 the complementary methods utilize only the initial or/and the terminal states. Neglecting the  
 257 intermediate states results in an imprecise partition, as was illustrated in Fig. 1 using a univariate  
 258 function, and even a reverse trend estimation (see  $\Delta R_{E_0}$  for Catchment NO. 1 in Table 3).

259 As with the LI method, the complementary method produced  $\Delta R_p$ ,  $\Delta R_{E_0}$ , and  $\Delta R_n$  that exactly  
 260 summed up to  $\Delta R$ . Although its resultant  $\Delta R_p$ ,  $\Delta R_{E_0}$ , and  $\Delta R_n$  values were all in accordance with the LI  
 261 method (Fig. 6), the LI method often yielded values beyond the bounds given by the complementary  
 262 method (Fig. 7); this is because the maximum or minimum sensitivities do not necessarily occur at the  
 263 initial or terminal states.

264  $\overline{\lambda_P}$ ,  $\overline{\lambda_{E_0}}$  and  $\overline{\lambda_n}$  imply the average runoff change induced by a unit change in  $P$ ,  $E_0$  and  $n$ ,  
 265 respectively (Appendix D).  $\overline{\lambda_P}$ ,  $\overline{\lambda_{E_0}}$  and  $\overline{\lambda_n}$  all varied by up to several times or even ten folds between  
 266 the studied catchments (Table S4). Fig. 8 shows that Eq. (2) reproduced  $\overline{\lambda_P}$ ,  $\overline{\lambda_{E_0}}$  and  $\overline{\lambda_n}$  very well  
 267 taking the long-term means of  $P$ ,  $E_0$ , and  $n$  as inputs, a fact that the dependent variable approached its  
 268 average if the independent variables were set to be their averages. This finding is of relevance to the  
 269 spatial prediction of  $\overline{\lambda_P}$ ,  $\overline{\lambda_{E_0}}$  and  $\overline{\lambda_n}$ .

270

### 271 4 Discussion

272 The LI method highlights the role of the evolutionary path in determining the resultant partition.  
 273 Yet, it seems that no studies have accounted for the path issue while evaluating the relative influences  
 274 of drivers. The limit of the LI method is high data requirement for obtaining the evolutionary path.  
 275 When the path data are unavailable, the complementary method can be considered as an alternative. The  
 276 complementary method is free of residuals; moreover, it employs both data of the reference and the



277 evaluation periods, thereby generally yielding sensitivities closer to the path-averaged results than the  
278 total differentiae method.

279 While using the Budyko models, a reasonable time scale is relevant to meet the assumption that  
280 changes in catchment water storage are small relative to the magnitude of fluxes of  $P$ ,  $R$  and  $E$   
281 (Donohue *et al.*, 2007; Roderick and Farquhar, 2011). A seven-year time scale was used in the present  
282 study, as most studies have suggested that a time period of 5-10 years (Zhang *et al.*, 2001; Zhang *et al.*,  
283 2016; Wu *et al.*, 2017a; Wu *et al.*, 2017b; Li *et al.*, 2017) or even one year (Roderick and Farquhar,  
284 2011; Sivapalan *et al.*, 2011; Carmona *et al.*, 2014; Ning *et al.*, 2017) is reasonable. Nevertheless, some  
285 studies argued that the time period should be longer than ten years (Li *et al.*, 2016; Dey and Mishra,  
286 2017). Using the Gravity Recovery and Climate Experiment (GRACE) satellite gravimetry, Zhao *et al.*  
287 (2011) detected the water storage variations for three largest river basins of China, namely, the Yellow,  
288 Yangtze, and Zhujiang. The Yellow River mostly drains an arid and semiarid region ( $P$ ,  $450 \cdot 10^{-3}\text{m}$ ;  $R$ ,  
289  $70 \cdot 10^{-3}\text{m}$ ;  $E$ ,  $380 \cdot 10^{-3}\text{m}$ ), and the Yangtze ( $P$ ,  $110 \cdot 10^{-3}\text{m}$ ;  $R$ ,  $550 \cdot 10^{-3}\text{m}$ ;  $E$ ,  $550 \cdot 10^{-3}\text{m}$ ) and the Zhujiang  
290 river basins ( $P$ ,  $1400 \cdot 10^{-3}\text{m}$ ;  $R$ ,  $780 \cdot 10^{-3}\text{m}$ ;  $E$ ,  $620 \cdot 10^{-3}\text{m}$ ) are humid. The amplitude of the water storage  
291 variations between years were 7, 37.2, and  $65 \cdot 10^{-3}\text{m}$  for the three rivers respectively, at one magnitude  
292 order smaller than the fluxes of  $P$ ,  $R$  and  $E$ . Although the observations cannot be directly extrapolated to  
293 other regions, the possibility seems remote that the use of a 7-year aggregated time strongly violates the  
294 assumption of the steady state condition.

295 The mutual independence between the drivers is crucial for a valid partition. In the present study,  
296 although annual  $P$  and  $E_0$  exhibited significant correlation for most catchments ( $p < 0.05$ ), the aggregated  
297  $P$ ,  $E_0$  and  $n$  over a 7-year period showed minimal correlation (mostly  $p > 0.1$ ). The interdependence  
298 between the drivers can considerably confound the resultant partitions of the LI method and other  
299 existing methods.

300 The LI method revises the concept of sensitivity at a point as the path-averaged sensitivity.  
301 Mathematically, the LI method is unrelated to a functional form and hence applies to communities other  
302 than just hydrology. For example, identifying the carbon emission budgets (an allowable amount of  
303 anthropogenic  $\text{CO}_2$  emission consistent with a limiting warming target), is crucial for global efforts to  
304 mitigate climate change. The LI method suggested that the emission budgets depends on both the  
305 emission magnitude and pathway (timing of emissions), which is in line with a recent study by Gasser  
306 *et al.* (2018). An optimal pathway would facilitate an elevated carbon budget unless the carbon-climate  
307 system behaves in a linear fashion.

308 This study presented the LI method using time-series data, but it applies equally to the case of  
309 spatial series of data. Given a model that relates fluvial or aeolian sediment load to the influencing  
310 factors (e.g. rainfall and topography), for example, the LI method can be used to separate their  
311 contributions to the sediment-load change along a river or in the along-wind direction.

## 313 5 Conclusions

314 Based on the line integral, I created a mathematically precise method to partition the synergistic  
315 effects of several factors that cumulatively drive a system to change from a state to the other. The  
316 method is relevant for quantitative assessments of the relative roles of the factors on the change in the

system state. I applied the LI method to partition the effects of climatic and catchment conditions on runoff within the Budyko framework. The method reveals that in addition to the change magnitude, the change pathways of climatic and catchment conditions also play a role. Instead of using the runoff sensitivity at a point, the LI method uses the path-averaged sensitivity, thereby ensuring a mathematically precise partition. As a mathematically accurate scheme, the LI method has the potential to be a generic attribution approach in the environmental sciences.

### Data availability

The data used in this study are freely available by contacting the authors.

### Author contribution

MZ designed the study, analyzed the data and wrote the manuscript.

### Competing interests

The authors declare that they have no conflict of interest.

### Appendix A: Mathematical proof of $\Delta z = \int_L f_x(x, y)dx + \int_L f_y(x, y)dy$

We define that the curve  $L$  in Fig. 3 is given by a parametric equation:  $x = x(t)$ ,  $y = y(t)$ ,  $t \in [t_0, t_N]$ , then  $\Delta z = z_N - z_0 = f[x(t_N), y(t_N)] - f[x(t_0), y(t_0)]$ . Substituting the parametric equations, we obtain:

The right-hand side of the equation =  $\int_L f_x(x, y)dx + \int_L f_y(x, y)dy$

$$= \int_{t_0}^{t_N} f_x[x(t), y(t)]dx(t) + \int_{t_0}^{t_N} f_y[x(t), y(t)]dy(t)$$

$$= \int_{t_0}^{t_N} \{f_x[x(t), y(t)]x'(t) + f_y[x(t), y(t)]y'(t)\} dt \quad (A1)$$

Let  $g(t) = f[x(t), y(t)]$ , and after using the chain rule to differentiate  $g$  with respect to  $t$ , we obtain:

$$g'(t) = \frac{\partial g}{\partial x} \frac{dx}{dt} + \frac{\partial g}{\partial y} \frac{dy}{dt} = f_x[x(t), y(t)]x'(t) + f_y[x(t), y(t)]y'(t) \quad (A2)$$

Thus,  $g'(t)$  is just the integrand in Eq. (A1), and Eq. (A1) can then be rewritten as:

$$\begin{aligned} \text{The right-hand side of the equation} &= \int_{t_0}^{t_N} g'(t) dt = [g(t)]_{t_0}^{t_N} = g(t_N) - g(t_0) \\ &= f[x(t_N), y(t_N)] - f[x(t_0), y(t_0)] = \text{The left-hand side of the equation} \end{aligned}$$

### Appendix B: The sum of $\int_L f_x(x, y)dx$ and $\int_L f_y(x, y)dy$ is path-independent

**Theorem:** Given an open simply-connected region  $G$  (i.e., no holes in  $G$ ) and two functions  $P(x, y)$  and  $Q(x, y)$  that have continuous first-order derivatives, if and only if  $\partial P / \partial y = \partial Q / \partial x$  throughout  $G$ ,

348 then  $\int_L P(x, y)dx + \int_L Q(x, y)dy$  is path independent, *i.e.*, it depends solely on the starting and ending  
 349 point of  $L$ .

350 We have  $\partial f_x / \partial y = \partial^2 z / \partial x \partial y$  and  $\partial f_y / \partial x = \partial^2 z / \partial y \partial x$ . As  $\partial^2 z / \partial x \partial y = \partial^2 z / \partial y \partial x$ , we can state that  
 351  $\partial f_x / \partial y = \partial f_y / \partial x$ , meeting the above condition and proving that  $\int_L f_x(x, y)dx + \int_L f_y(x, y)dy$  is path  
 352 independent. The statement was further exemplified using a fictitious example in Appendix C.

### 353 **Appendix C: A fictitious example to show how the LI method works**

354 Runoff ( $R$ ,  $10^{-3}\text{m yr}^{-1}$ ) at a site is assumed to increase from 120 to 195  $10^{-3}\text{m yr}^{-1}$  with  $\Delta R = 75 \cdot 10^{-3}$   
 355  $\text{m yr}^{-1}$ ; meanwhile, precipitation ( $P$ ,  $10^{-3}\text{m yr}^{-1}$ ) varies from 600 to 650  $10^{-3}\text{m yr}^{-1}$  ( $\Delta P = 75 \cdot 10^{-3}\text{m yr}^{-1}$ )  
 356 and the runoff coefficient ( $C_R$ , dimensionless) varies from 0.2 to 0.3 ( $\Delta C_R = 0.1$ ). The goal is to partition  
 357  $\Delta R$  into the effects of the precipitation ( $\Delta R_P$ ) and runoff coefficient ( $\Delta R_{C_R}$ ), provided that  $P$  and  $C_R$  are  
 358 independent. We have a function  $R = PC_R$  and its partial derivatives  $\partial R / \partial P = C_R$  and  $\partial R / \partial C_R = P$ . Given a  
 359 path  $L$  along which  $P$  and  $C_R$  change and using Eq. (3), the LI method evaluates  $\Delta R_P$  and  $\Delta R_{C_R}$  as:

$$360 \Delta R_{C_R} = \int_L \partial R / \partial C_R dC_R = \int_L P dC_R \text{ and } \Delta R_P = \int_L \partial R / \partial P dP = \int_L C_R dP \quad (C1)$$

361 The result differs depending on  $L$  but the sum of  $\Delta R_P$  and  $\Delta R_{C_R}$  uniformly equals  $\Delta R$ . This  
 362 dynamic is demonstrated using Fig. 3, in which we considered that the  $x$ -axis represents  $C_R$  and the  $y$ -  
 363 axis  $P$ . Point A denotes the initial state ( $C_R = 0.2, P = 600$ ) and point C the terminal state ( $C_R = 0.3, P =$   
 364  $650$ ). I calculated  $\Delta R_P$  and  $\Delta R_{C_R}$  along three fictitious paths as follows:

365 1)  $L=AC$ . Line segment AC has equation  $P = 500C_R + 500, 0.2 \leq C_R \leq 0.3$ . Let's take  $C_R$  as the  
 366 parameter and write the equation in the parametric form as  $P = 500C_R + 500, C_R = C_R, 0.2 \leq C_R \leq 0.3$ . By  
 367 substituting the equation into Eq. (C1), we have:

$$368 \Delta R_{C_R} = \int_{AC} P dC_R = \int_{0.2}^{0.3} (500C_R + 500) dC_R = 62.5$$

$$369 \Delta R_P = \int_{AC} C_R dP = \int_{AC} C_R d(500C_R + 500) = 500 \int_{0.2}^{0.3} C_R dC_R = 12.5$$

370 2)  $L=AB+BC$ . To evaluate on the broken line, we can evaluate separately on AB and BC and then sum  
 371 them up. The equation for AB is  $P = 600, 0.2 \leq C_R \leq 0.3$ , while for BC is  $C_R = 0.3, 600 \leq P \leq 650$ . Notes  
 372 that a constant  $C_R$  or  $P$  implies that  $dC_R = 0$  or  $dP = 0$ . Eq. (C1) then becomes:

$$373 \Delta R_{C_R} = \int_{AB+BC} P dC_R = \int_{AB} P dC_R + \int_{BC} P dC_R = \int_{0.2}^{0.3} 600 dC_R + 0 = 60$$

$$374 \Delta R_P = \int_{AB+BC} C_R dP = \int_{AB} C_R dP + \int_{BC} C_R dP = 0 + \int_{600}^{650} 0.3 dP = 15$$

375 3)  $L=AD+DC$ . The equation for AD is  $C_R = 0.2, 600 \leq P \leq 650$  and is  $P = 650, 0.2 \leq C_R \leq 0.3$  for DC.  
 376  $\Delta R_P$  and  $\Delta R_{C_R}$  are evaluated as:

$$377 \Delta R_{C_R} = \int_{AD+DC} P dC_R = \int_{AD} P dC_R + \int_{DC} P dC_R = 0 + \int_{0.2}^{0.3} 650 dC_R = 65$$

$$378 \Delta R_P = \int_{AD+DC} C_R dP = \int_{AD} C_R dP + \int_{DC} C_R dP = \int_{600}^{650} 0.2 dP + 0 = 10$$

379 As expected, the sum of  $\Delta R_P$  and  $\Delta R_{C_R}$  persistently equals  $\Delta R$  although  $\Delta R_P$  and  $\Delta R_{C_R}$  varies with  $L$ .

### 381 Appendix D: Mathematical proof of the path-averaged sensitivity

382 If the interval  $[x_0, x_N]$  in Fig. 3 is partitioned into  $N$  distinct bins of the same width  $\Delta x_i = \Delta x/N$ . Eq.  
383 (3a) can then be rewritten as:

$$384 \quad \Delta Z_x = \int_L f_x(x, y) dx = \lim_{\tau \rightarrow 0} \sum_{i=0}^{N-1} f_x(x_i, y_i) \Delta x_i = \lim_{\tau \rightarrow 0} N \Delta x_i \frac{\sum_{i=0}^{N-1} f_x(x_i, y_i)}{N} = \Delta x \lim_{\tau \rightarrow 0} \frac{\sum_{i=0}^{N-1} f_x(x_i, y_i)}{N} = \overline{\lambda_x} \Delta x$$

385 where  $\overline{\lambda_x} = \lim_{\tau \rightarrow 0} \frac{\sum_{i=1}^N f_x(x_i, y_i)}{N}$ , denoting the average of  $f_x(x, y)$  along the curve  $L$ . Likewise, we have

386  $\Delta Z_y = \overline{\lambda_y} \Delta y$ , where  $\overline{\lambda_y}$  denotes the average of  $f_y(x, y)$  along the curve  $L$ . As a result:

$$387 \quad \Delta Z = \overline{\lambda_x} \Delta x + \overline{\lambda_y} \Delta y \quad (\text{D1})$$

388 The result can readily be extended to a function of three variables. Applying the mathematic  
389 derivation determined above to the MCY equation results in a precise form of Eq. (7):

$$390 \quad \Delta R = \Delta R_P + \Delta R_{E_0} + \Delta R_n = \overline{\lambda_P} \Delta P + \overline{\lambda_{E_0}} \Delta E_0 + \overline{\lambda_n} \Delta n, \quad (\text{D2})$$

391 where  $\Delta R_P = \overline{\lambda_P} \Delta P$ ,  $\Delta R_{E_0} = \overline{\lambda_{E_0}} \Delta E_0$ ,  $\Delta R_n = \overline{\lambda_n} \Delta n$ , and  $\overline{\lambda_P}$ ,  $\overline{\lambda_{E_0}}$  and  $\overline{\lambda_n}$  denote the arithmetic mean of  $\partial R / \partial P$ ,  
392  $\partial R / \partial E_0$ , and  $\partial R / \partial n$  along a path of climate and catchment changes, respectively. Because  $\overline{\lambda_P} = \Delta R_P / \Delta P$ ,  
393  $\overline{\lambda_{E_0}} = \Delta R_{E_0} / \Delta E_0$ , and  $\overline{\lambda_n} = \Delta R_n / \Delta n$ ,  $\overline{\lambda_P}$ ,  $\overline{\lambda_{E_0}}$  and  $\overline{\lambda_n}$  also imply the runoff change due to a unit change in  $P$ ,  
394  $E_0$  and  $n$ , respectively.

395

### 396 Appendix E: Path-averaged sensitivity in one-dimensional cases

397 Given a one-dimensional function  $z=f(x)$  and its derivative  $f'(x)$ . We assumed that  $f'(x)$

398 averages  $\overline{\lambda_x}$  over the range  $(x, x + \Delta x)$ , i.e.  $\overline{\lambda_x} = \lim_{\tau \rightarrow 0} \frac{\sum_{i=1}^N f'(x_i)}{N}$ . According to the mean value theorem for

399 integrals,  $\overline{\lambda_x} = \int_x^{x+\Delta x} f'(x) dx / \Delta x$ . In terms of the Newton-Leibniz formula,

400  $\int_x^{x+\Delta x} f'(x) dx = f(x + \Delta x) - f(x) = \Delta z$ . Thus, we obtain:  $\overline{\lambda_x} = \Delta z / \Delta x$ .

401

### 402 Acknowledgments

403 This work was funded by the National Natural Science Foundation of China (41671278), the GDAS'  
404 Project of Science and Technology Development (2019GDASYL-0103043) and (2019GDASYL-  
405 0502004). I thank Mr. Y.Q. Zheng for his assistance with the mathematic derivations.

407 **References**

- 408 Barnett, T. P., Pierce, D. W., Hidalgo, H. G., Bonfils, C., Santer, B. D., Das, T., Bala G., Woods, A. W.,  
 409 Nozawa, T., Mirin, A. A., Cayan D. R., and M. D. Dettinger: Human-induced changes in the  
 410 hydrology of the western United States. *Science*, 319(5866), 1080-1083.  
 411 <https://doi.org/10.1126/science.1152538>, 2008.
- 412 Berghuijs, W. R., R. A. Woods: Correspondence: Space-time asymmetry undermines water yield  
 413 assessment. *Nature Communications* 7, 11603. <https://doi.org/10.1038/ncomms11603>, 2016.
- 414 Binley, A. M., Beven, K. J., Calver, A., and L. G. Watts: Changing responses in hydrology: assessing  
 415 the uncertainty in physically based model predictions. *Water Resources Research*, 27(6), 1253-1261.  
 416 <https://doi.org/10.1029/91WR00130>, 1991.
- 417 Brown, A. E., Zhang, L., McMahon, T. A., Western, A. W. and R. A. Vertessy: A review of paired  
 418 catchment studies for determining changes in water yield resulting from alterations in vegetation.  
 419 *Journal of Hydrology*, 310, 26–61. <https://doi.org/10.1016/j.jhydrol.2004.12.010>, 2005.
- 420 Budyko, M. I.: *Climate and Life*. Academic, N. Y. 1974.
- 421 Carmona, A. M., Sivapalan, M., Yaeger, M. A., and Poveda, G.: Regional patterns of interannual  
 422 variability of catchment water balances across the continental US: A Budyko framework. *Water*  
 423 *Resources Research*, 50, 9177–9193. <https://doi:10.1002/2014wr016013>, 2014.
- 424 Choudhury, B. J.: Evaluation of an empirical equation for annual evaporation using field observations  
 425 and results from a biophysical model. *Journal of Hydrology*, 216, 99–110.  
 426 [https://doi.org/10.1016/S0022-1694\(98\)00293-5](https://doi.org/10.1016/S0022-1694(98)00293-5), 1999.
- 427 Dey, P., and A. Mishra: Separating the impacts of climate change and human activities on streamflow:  
 428 A review of methodologies and critical assumptions. *Journal of Hydrology*, 548, 278-290.  
 429 <https://doi.org/10.1016/j.jhydrol.2017.03.014>, 2017.
- 430 Donohue, R. J., M. L. Roderick, and T. R. McVicar: On the importance of including vegetation  
 431 dynamics in Budyko's hydrological model. *Hydrology and Earth System Sciences*, 11, 983–995.  
 432 <https://doi.org/10.5194/hess-11-983-2007>, 2007.
- 433 Gao, G., Ma, Y., and B. Fu: Multi-temporal scale changes of streamflow and sediment load in a loess  
 434 hilly watershed of China. *Hydrological Processes*, 30(3), 365-382, [10.1002/hyp.10585](https://doi.org/10.1002/hyp.10585), 2016.
- 435 Gasser, T., M. Kechiar, P. Ciais, E. J. Burke, T. Kleinen, D. Zhu, Y. Huang, A. Ekici, and M.  
 436 Obersteiner: Path-dependent reductions in CO<sub>2</sub> emission budgets caused by permafrost carbon  
 437 release. *Nature Geoscience*, 11, 830–835. <https://doi.org/10.1038/s41561-018-0227-0>, 2018.
- 438 Jiang, C., Xiong, L., Wang, D., Liu, P., Guo, S., and Xu C.: Separating the impacts of climate change  
 439 and human activities on runoff using the Budyko-type equations with time-varying parameters.  
 440 *Journal of Hydrology*, 522, 326-338, [10.1016/j.jhydrol.2014.12.060](https://doi.org/10.1016/j.jhydrol.2014.12.060), 2015.
- 441 Li, Z., Ning, T., Li, J., and D. Yang: Spatiotemporal variation in the attribution of streamflow changes  
 442 in a catchment on China's Loess Plateau. *Catena*, 158:1–8.  
 443 <https://doi.org/10.1016/j.catena.2017.06.008>, 2017.
- 444 Liang, W., D. Bai, F. Wang, B. Fu, J. Yan, S. Wang, Y. Yang, D. Long, and M. Feng: Quantifying the  
 445 impacts of climate change and ecological restoration on streamflow changes based on a Budyko

446 hydrological model in China's Loess Plateau. *Water Resources Research*, 51, 6500–6519.  
447 <https://doi.org/10.1002/2014WR016589>, 2015.

448 Liu, J., Zhang, Q., Singh, V. P., and P. Shi. Contribution of multiple climatic variables and human  
449 activities to streamflow changes across China. *Journal of Hydrology*, 545, 145-162.  
450 <https://doi.org/10.1016/j.jhydrol.2016.12.016>, 2016.

451 Mezentsev, V. S.: More on the calculation of average total evaporation. *Meteorol. Gidrol.*, 5, 24–26,  
452 1955.

453 Ning, T., Li, Z., and W. Liu: Vegetation dynamics and climate seasonality jointly control the  
454 interannual catchment water balance in the Loess Plateau under the Budyko framework,  
455 *Hydrology and Earth System Sciences*, 21, 1515-1526. <https://doi.org/10.5194/hess-2016-484>, 2017.

456 Roderick, M. L., and G. D. Farquhar: A simple framework for relating variations in runoff to variations  
457 in climatic conditions and catchment properties. *Water Resources Research*, 47, W00G07,  
458 <https://doi.org/10.1029/2010WR009826>, 2011.

459 Sankarasubramanian, A., R. M. Vogel, and J. F. Limbrunner: Climate elasticity of streamflow in the  
460 United States. *Water Resources Research*, 37(6), 1771-1781.  
461 <https://doi.org/10.1029/2000WR900330>, 2001.

462 Schaake, J. C.: From climate to flow. *Climate Change and U.S. Water Resources*, edited by P. E.  
463 Waggoner, chap. 8, pp. 177 - 206, John Wiley, N. Y. 1990.

464 Sivapalan, M., Yaeger, M. A., Harman, C. J., Xu, X. Y., and P. A. Troch: Functional model of water  
465 balance variability at the catchment scale: 1. Evidence of hydrologic similarity and space-time  
466 symmetry, *Water Resources Research*, 47, W02522, doi:10.1029/2010wr009568, 2011.

467 Sposito, G.: Understanding the Budyko equation. *Water*, 9(4), 236. <https://doi.org/10.3390/w9040236>,  
468 2017.

469 Sun, Y., Tian, F., Yang, L., and H. Hu: Exploring the spatial variability of contributions from climate  
470 variation and change in catchment properties to streamflow decrease in a mesoscale basin by three  
471 different methods. *Journal of Hydrology*, 508(2), 170-180,  
472 <https://doi.org/10.1016/j.jhydrol.2013.11.004>, 2014.

473 Wang, D., and M. Hejazi: Quantifying the relative contribution of the climate and direct human impacts  
474 on mean annual streamflow in the contiguous United States. *Water Resources Research*, 47, W00J12,  
475 <https://doi.org/10.1029/2010WR010283>, 2011.

476 Wang, W., Q. Shao, T. Yang, S. Peng, W. Xing, F. Sun, and Y. Luo: Quantitative assessment of the  
477 impact of climate variability and human activities on runoff changes: A case study in four  
478 catchments of the Haihe River basin, China. *Hydrological Processes*, 27(8), 1158–1174.  
479 <https://doi.org/10.1002/hyp.9299>, 2013.

480 Wu, J., Miao, C., Wang, Y., Duan, Q., and X. Zhang: Contribution analysis of the long-term changes in  
481 seasonal runoff on the Loess Plateau, China, using eight Budyko-based methods. *Journal of*  
482 *hydrology*, 545, 263-275. <https://doi.org/10.1016/j.jhydrol.2016.12.050>, 2017a.

483 Wu, J., Miao, C., Zhang, X., Yang, T., and Q. Duan: Detecting the quantitative hydrological response to  
484 changes in climate and human activities. *Science of the Total Environment*, 586, 328-337.  
485 <https://doi.org/10.1016/j.scitotenv.2017.02.010>, 2017b.

486 Xu, X., Yang, D., Yang, H. and Lei, H.: Attribution analysis based on the Budyko hypothesis for  
487 detecting the dominant cause of runoff decline in Haihe basin. *Journal of Hydrology*, 510: 530-540.

488 <http://dx.doi.org/10.1016/j.jhydrol.2013.12.052>, 2014.

489 Yang, H., D. Yang, Z. Lei, and F. Sun: New analytical derivation of the mean annual water-energy  
490 balance equation. *Water Resources Research*, 44, W03410. <https://doi.org/10.1029/2007WR006135>,  
491 2008.

492 Yang, H., and D. Yang: Derivation of climate elasticity of runoff to assess the effects of climate change  
493 on annual runoff. *Water Resources Research*, 47, W07526. <https://doi.org/10.1029/2010WR009287>,  
494 2011.

495 Yang, H., D. Yang, and Q. Hu: An error analysis of the Budyko hypothesis for assessing the  
496 contribution of climate change to runoff. *Water Resources Research*, 50, 9620–9629.  
497 <https://doi.org/10.1002/2014WR015451>, 2014.

498 Zhao, Q. L., Liu, X. L., Ditmar, P., Siemes, C., Revtova, E., Hashemi-Farahani, H., and R. Klees: Water  
499 storage variations of the Yangtze, Yellow, and Zhujiang river basins derived from the DEOS Mass  
500 Transport (DMT-1) model. *Science China-Earth Sciences*, 54, 667-677.  
501 <https://doi.org/10.1007/s11430-010-4096-7>, 2011.

502 Zhang, S., H. Yang, D. Yang, and A. W. Jayawardena: Quantifying the effect of vegetation change on  
503 the regional water balance within the Budyko framework. *Geophysical Research Letters*, 43, 1140–  
504 1148. <https://doi.org/10.1002/2015GL066952>, 2016.

505 Zhang, L., Dawes, W. R. and G. R. Walker: Response of mean annual evapotranspiration to vegetation  
506 changes at catchment scale. *Water Resources Research* 37, 701–708. doi; 10.1029/2000WR900325,  
507 2001.

508 Zhang, L., F. Zhao, A. Brown, Y. Chen, A. Davidson, and R. Dixon: Estimating Impact of Plantation  
509 Expansions on Streamflow Regime and Water Allocation. CSIRO Water for a Healthy Country,  
510 Canberra, Australia. 2010.

511 Zhang, L., F. Zhao, Y. Chen, and R. N. M. Dixon: Estimating effects of plantation expansion and  
512 climate variability on streamflow for catchments in Australia. *Water Resources Research*, 47,  
513 W12539, <https://doi.org/10.1029/2011WR010711>, 2011.

514 Zheng, H., L. Zhang, R. Zhu, C. Liu, Y. Sato, and Y. Fukushima: Responses of streamflow to climate  
515 and land surface change in the headwaters of the Yellow River Basin. *Water Resources Research*, 45,  
516 W00A19. <https://doi.org/10.1029/2007WR006665>, 2009.

517 Zhou, S., B. Yu, L. Zhang, Y. Huang, M. Pan, and G. Wang (2016), A new method to partition climate  
518 and catchment effect on the mean annual runoff based on the Budyko complementary relationship.  
519 *Water Resources Research*, 52, 7163–7177. <https://doi.org/10.1002/2016WR019046>, 2016.

520  
521  
522  
523  
524  
525  
526  
527  
528  
529  
530

531 **Table 1.** Summary of the long-term hydrometeorological characteristics of the selected catchments<sup>a</sup>

Catchment No. <sup>b</sup>	Area (10 <sup>6</sup> m <sup>2</sup> )	<i>R</i>	<i>P</i>	<i>E</i> <sub>0</sub>	<i>n</i>	<i>AI</i>	Reference Period	Evaluation Period	The final Subperiod
1	391	218	1014	935	3.5	0.92	1933-1955	1956-2008	1998-2008
2	16.64	32.9	634	1087	3.16	1.71	1979-1984	1985-2008	1999-2008
3	559	183	787	780	2.68	0.99	1960-1978	1979-2000	1993-2000
4	606	73	729	998	3.07	1.37	1971-1995	1996-2009	2003-2009
5	760	77.9	689	997	2.66	1.45	1970-1995	1996-2009	2003-2009
6	502	57.2	730	988	3.59	1.35	1974-1995	1996-2008	1996-2008
7	673	431	1013	953	1.34	0.94	1947-1955	1956-2008	1998-2008
8	390	139	840	1021	2.61	1.22	1966-1980	1981-2005	1995-2005
9	1130	20.7	633	1077	3.79	1.7	1972-1982	1983-2007	1997-2007
10	89	272	963	826	2.82	0.86	1958-1965	1966-1999	1987-1999
11	243	38.5	735	1010	4.27	1.37	1989-1995	1996-2007	1996-2007
12	56.35	65.8	744	1007	3.35	1.35	1989-1995	1996-2008	1996-2008
13	14484	385	893	1022	1.11	1.14	1970-1989	1990-2000	1990-2000
14	38625	461	985	1087	1.03	1.1	1970-1989	1990-2000	1990-2000
15	59115	388	897	1161	1.02	1.29	1970-1989	1990-2000	1990-2000
16	95217	371	881	1169	1.03	1.33	1970-1989	1990-2000	1990-2000
17	121,972	171	507	768	1.17	1.52	1960-1990	1991-2000	1991-2000
18	106,500	60.5	535	905	2.25	1.69	1960-1970	1971-2009	1999-2009
19	5891	34.4	506	964	2.54	1.91	1952-1996	1997-2011	2004-2011

532 <sup>a</sup>*R*, *P*, and *E*<sub>0</sub> represent the mean annual runoff, precipitation and potential evaporation, all in 10<sup>-3</sup>m yr<sup>-1</sup>.  
533 *n* (dimensionless) is the parameter representing catchment properties in the MCY equation. *AI* is the  
534 dimensionless aridity index ( $AI = E_0/P$ ). Data of Catchments 1-12 were derived from Zhang *et al.*  
535 (2010). Data of Catchments 13-16 were from Sun *et al.* (2014). Data of Catchments 17-19 were from  
536 Zheng *et al.* (2009), Jiang *et al.* (2015), and Gao *et al.* (2016), respectively. I used the change points  
537 given in the literatures to divide the observation period into the reference and elevation periods. The LI  
538 method further divides the evaluation period into a number of subperiods. The column “The final  
539 Subperiod” denotes the final subperiod, which was used as the evaluation period for the total  
540 differential method, the decomposition method and the complementary method.

541 <sup>b</sup>Catchments 1-12 are in Australia and the others are in China. 1: Adjungbilly CK; 2: Batalling Ck; 3:  
542 Bombala River; 4: Crawford River; 5: Darlot Ck; 6: Eumeralla River; 7: Goobarragandra CK; 8:  
543 Jingellic CK; 9: Mosquito CK; 10: Traralgon Ck; 11: Upper Denmark River; 12: Yate Flat Ck; 13:  
544 Yangxian station, Hang River; 14: Ankang station, Hang River; 15: Baihe station, Hang River; 16:  
545 Danjiangkou station, Hang River; 17: Headwaters of the Yellow River Basin; 18: Wei River; 19: Yan  
546 River.

547  
548  
549  
550



551  
552

**Table 2.** Comparisons of  $R$  (mm yr<sup>-1</sup>),  $P$  (mm yr<sup>-1</sup>),  $E_0$  (mm yr<sup>-1</sup>), and  $n$  (dimensionless) between the reference and the evaluation periods<sup>a</sup>

Catchment No.	$R_1$	$R_2$	$P_1$	$P_2$	$E_{01}$	$E_{02}$	$n_1$	$n_2$	$\Delta R$	$\Delta P$	$\Delta E_0$	$\Delta n$
1	223	216	959	1038	950	928	2.7	4.1	-7.2	79.2	-21	1.4
2	40.6	31	655	629	1087	1087	3	3.2	-9.7	-27	0	0.2
3	249	127	847	736	780	780	2.3	3.2	-122	-112	0.4	0.9
4	90.6	41.5	753	685	1002	989	2.9	3.7	-49	-67	-13	0.8
5	94.9	46.3	718	633	1000	992	2.5	3	-49	-85	-9	0.5
6	70.8	34.3	756	687	989	987	3.4	4.1	-36	-69	-2	0.6
7	575	406	1123	995	931	957	1.1	1.4	-169	-128	25	0.3
8	139	139	871	821	1043	1008	2.7	2.5	-0.4	-50	-35	-0.2
9	24.1	19.2	659	621	1100	1067	3.7	3.8	-4.9	-37	-33	0.1
10	301	265	992	956	820	828	2.7	2.8	-36	-36	7.4	0.1
11	48.5	32.6	752	725	991	1021	4.2	4.4	-16	-28	30	0.2
12	90.4	52.6	753	739	991	1015	2.9	3.7	-38	-14	24	0.8
13	435	295	948	795	1008	1047	1.1	1.2	-139	-153	38	0.1
14	520	353	1035	894	1074	1109	1	1.2	-167	-141	35	0.2
15	441	291	939	820	1149	1182	1	1.2	-151	-119	33	0.2
16	412	296	913	821	1163	1179	1	1.1	-116	-92	15	0.2
17	180	144	512	491	774	751	1.1	1.3	-36	-21	-23	0.2
18	90.2	52.1	585	520	895	908	2.1	2.3	-38	-65	13	0.2
19	37.7	24.6	521	462	954	995	2.6	2.5	-13	-59	41	-0.1

553  
554  
555  
556  
557  
558  
559  
560  
561  
562  
563  
564  
565  
566  
567  
568  
569  
570  
571

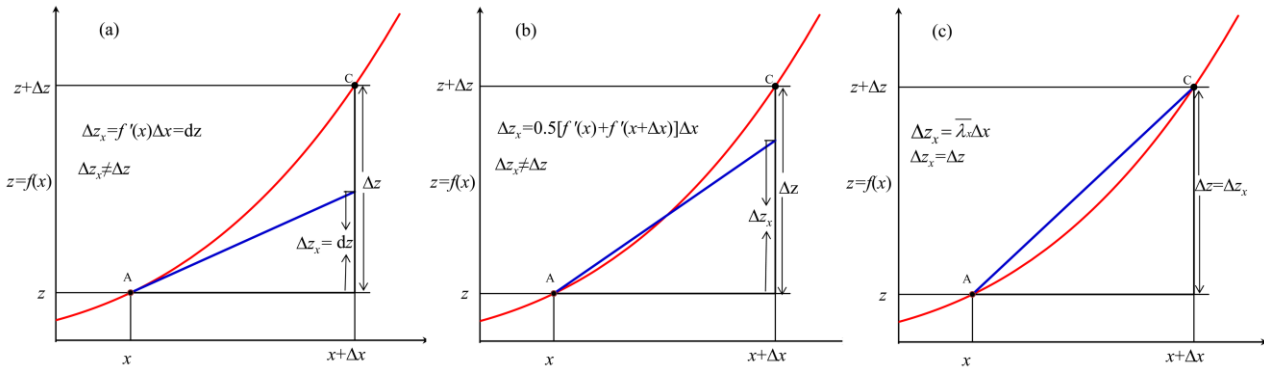
<sup>a</sup>The subscript "1" denotes the reference period and "2" denotes the evaluation period.  $\Delta X = X_2 - X_1$  ( $X$  as a substitute for  $R$ ,  $P$ ,  $E_0$ , and  $n$ ).

572  
573  
574

**Table 3.** Effects of precipitation ( $\Delta R_P$ ,  $10^{-3}\text{m yr}^{-1}$ ), potential evapotranspiration ( $\Delta R_{E_0}$ ,  $10^{-3}\text{m yr}^{-1}$ ), and catchment changes ( $\Delta R_n$ ,  $10^{-3}\text{m yr}^{-1}$ ) on the mean annual runoff determined from the four evaluated methods

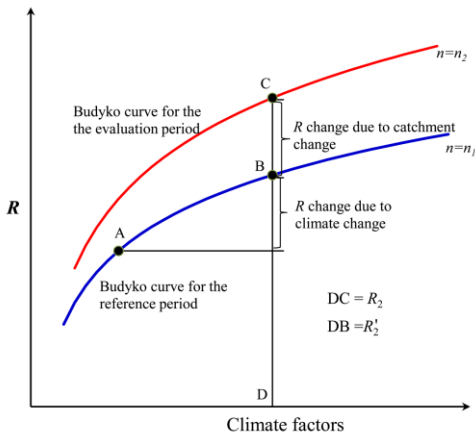
Catchment NO. <sup>a</sup>	LI Method			Decomposition Method	Total Differential Method			Complementary Method		
	$\Delta R_P$	$\Delta R_{E_0}$	$\Delta R_n$	$\Delta R_n$	$\Delta R_P$	$\Delta R_{E_0}$	$\Delta R_n$	$\Delta R_P$	$\Delta R_{E_0}$	$\Delta R_n$
1	-70.9	-8.99	-24.3	-44.6	-67	4.82	-62	-60.7	4.34	-47.3
2	-6.49	0.95	-9.74	-9.65	-7.2	1.3	-13	-6.23	1.13	-10.2
3	-89	25.9	-140	-128	-104	26.6	-483	-88	25.7	-140
4	-18.1	2.09	-35.4	-36.3	-18	2.37	-58	-14.8	1.99	-38.5
5	-27.9	1.14	-21.3	-18.6	-34	1.18	-27	-28.1	0.97	-20.9
6	-19.9	0.29	-16.7	-14.9	-24	0.36	-22	-19.9	0.29	-16.7
7	-211	-7.19	-101	-90.9	-236	-6.9	-134	-211	-6.21	-102
8	-32.2	12.3	-14.4	-12.6	-35	12.6	-15	-32.9	11.9	-13.3
9	-11.8	3.02	-9.96	-8.45	-13	0.85	-20	-8.76	0.56	-10.5
10	-9.88	-3.99	-79.2	-82	-11	-0.5	-154	-10.8	-0.57	-81.6
11	-6.98	-4.36	-4.54	-4.21	-8	-5.1	-5.2	-7	-4.38	-4.51
12	-4.84	-4.42	-28.7	-27.9	-5.6	-5	-37	-4.85	-4.4	-28.6
13	-104	-8.56	-24.8	-23	-110	-9.4	-27	-103	-8.52	-25.1
14	-99.3	-7.99	-58.8	-56	-105	-8.3	-68	-99	-7.92	-59.1
15	-78.8	-6.26	-63.9	-61	-84	-6.5	-76	-78.6	-6.2	-64.2
16	-60.1	-2.79	-53.5	-52	-64	-2.9	-62	-60	-2.77	-53.6
17	-11.9	3.89	-27.6	-27	-12	3.81	-31	-11.9	3.85	-27.5
18	-27.5	-2.46	-18.5	-17	-31	-4.4	-26	-25.5	-3.47	-19.5
19	-10.4	-3.47	-2.11	-3.4	-9.9	-4.8	-4.8	-8.27	-3.86	-3.82

575  
576  
577  
578  
579  
580  
581  
582  
583  
584  
585  
586  
587  
588  
589  
590  
591



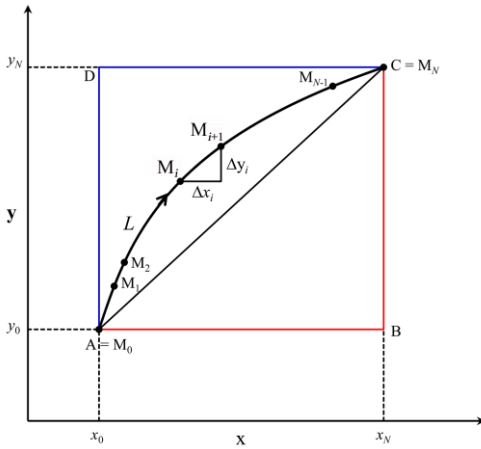
593  
 594  
 595  
 596  
 597  
 598  
 599

**Fig. 1.** For a non-linear function  $z=f(x)$ , the total differential method (a) and the complementary method (b) fails to accurately estimate the effect ( $\Delta z_x$ ) of  $x$  on  $z$  when  $x$  changes by  $\Delta x$ , but the LI method (c) does. For a univariate function, the  $z$  change is exclusively driven by  $x$ , so that  $\Delta z_x$  should be equal to  $\Delta z$ .  $\Delta z_x = \Delta z$  in (c) but not in (a) and (b).  $\bar{\lambda}_x$  in (c) represents the average sensitivity along the curve AC and  $\bar{\lambda}_x = \Delta z / \Delta x$ , see Appendix E for details.

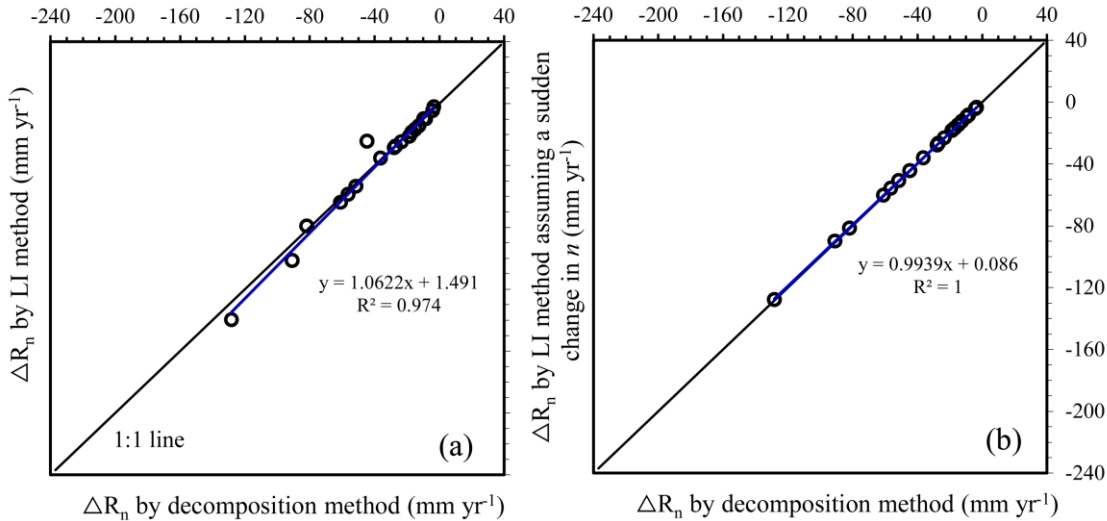


600  
 601  
 602  
 603  
 604  
 605  
 606

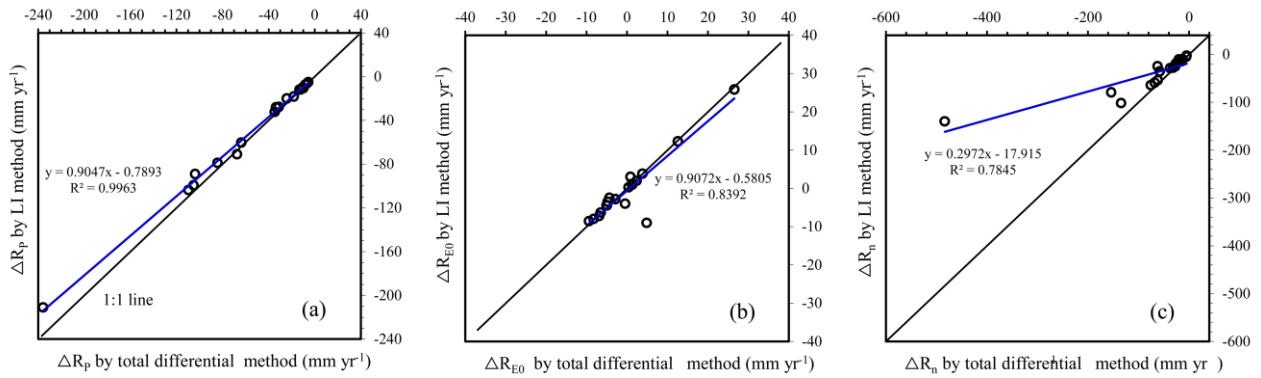
**Fig. 2.** A schematic plot to illustrate the decomposition method. Point A denotes the initial state (the reference period) and Point C denotes the terminal state (the evaluation period).  $R_2$  represents the mean annual runoff of the evaluation period, and  $R_2_1$  the mean annual runoff given the climate conditions of the evaluation period and the catchment conditions of the reference period. See Section 2.4 for details.



607  
608 **Fig. 3.** A schematic plot illustrating the LI method.  
609  
610

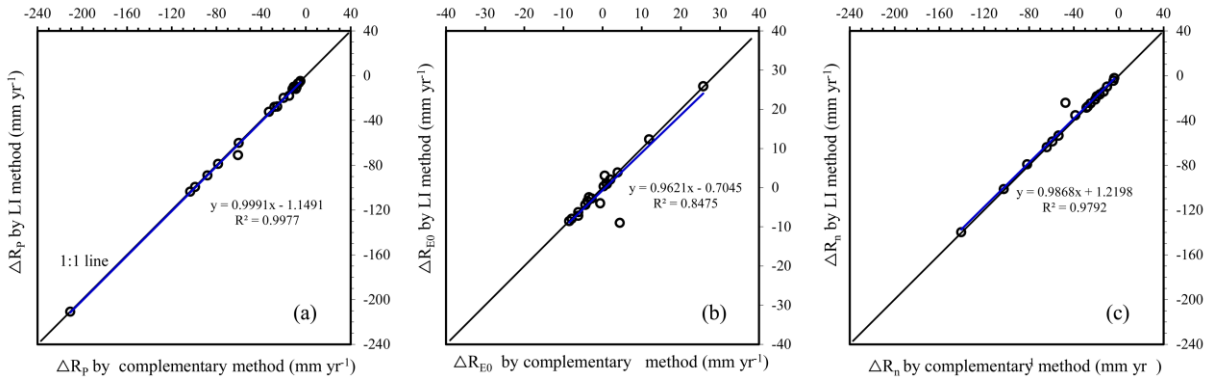


611  
612 **Fig. 4.** Comparisons between the LI method and the decomposition method. (a) Comparison of the  
613 estimated contributions to the runoff changes from the catchment changes ( $\Delta R_n$ ); (b) the decomposition  
614 method is equivalent to the LI method that assumes a sudden change in catchment properties following  
615 climate change. In this case, the integral path of the LI method can be considered as the path ABC in  
616 Fig. 3 ( $x$  represents climate factors and  $y$  catchment properties, *i.e.*  $n$ ) and  
617  $\Delta R_n = \int_{AB+BC} \frac{\partial R}{\partial n} dn = \int_{AB} \frac{\partial R}{\partial n} dn + \int_{BC} \frac{\partial R}{\partial n} dn = 0 + \int_{BC} \frac{\partial R}{\partial n} dn = \int_{n_1}^{n_2} f_n(P_2, E_{02}, n) dn$ , where the subscript "1"  
618 denotes the reference period and "2" denotes the final subperiod of the evaluation period.  
619  
620  
621  
622  
623



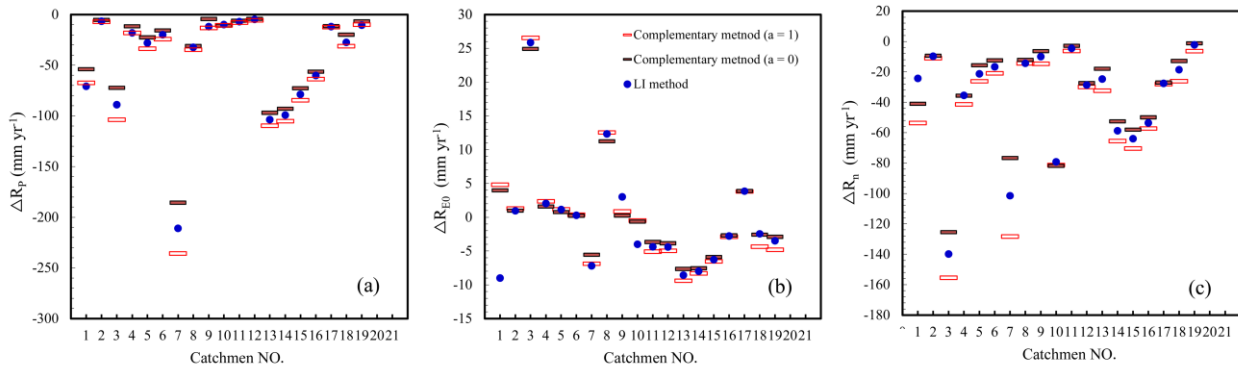
624  
625  
626  
627  
628

**Fig. 5.** Comparisons of the estimated contribution to runoff from the changes in (a) precipitation ( $\Delta R_P$ ), (b) potential evapotranspiration ( $\Delta R_{E_0}$ ), and (c) catchment properties ( $\Delta R_n$ ) between the LI method and the total differential method.



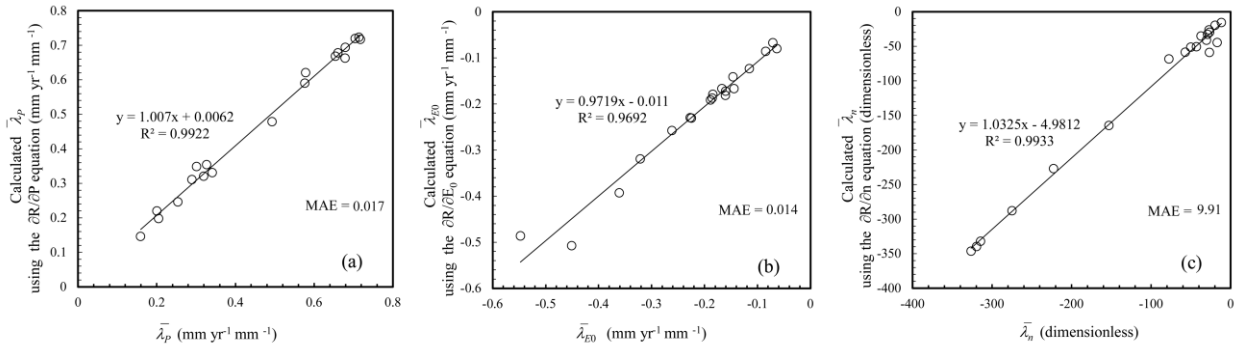
629  
630  
631  
632  
633

**Fig. 6.** Comparisons of (a)  $\Delta R_P$ , (b)  $\Delta R_{E_0}$ , and (c)  $\Delta R_n$  between the LI method and the complementary method ( $a = 0.5$ ).



634  
635  
636  
637  
638

**Fig. 7.** Comparisons of (a)  $\Delta R_P$ , (b)  $\Delta R_{E_0}$ , and (c)  $\Delta R_n$  by the LI method with the upper and lower bounds given by the complementary method. According to Zhou *et al.* (2016),  $\Delta R_P$ ,  $\Delta R_{E_0}$ , and  $\Delta R_n$  reach their bounds when  $a$  is 0 or 1.



639

640

**Fig. 8.** Performances of Eq. (2) to be used to predict  $\bar{\lambda}_P$ ,  $\bar{\lambda}_{E_0}$  and  $\bar{\lambda}_n$  with the long-term mean values

641

of  $P$ ,  $E_0$ , and  $n$  as inputs.  $MAE = N^{-1} \sum_{i=1}^N |O_i - P_i|$ , is the mean absolute error, where  $O$  and  $P$  are values

642

that actually encountered (given in Table S4) and predicted using Eq. (2) respectively, and  $N$  is the

643

number of selected catchments.

644

645